

Chapter 2

Bronze Sculptures and Lead Objects Tell Stories About Their Creators: Investigation of Renaissance Sculptures and Ancient Ingots by Means of Neutron Tomography

E.H. Lehmann, R. van Lang, M. Estermann, S. Hartmann,
F. LoCelso, N. Kardjilov, P. Tisseyre and S. Tusa

Abstract Renaissance bronze objects from the Rijksmuseum (Amsterdam) collection and lead ingots from ancient roman shipwrecks found near Sicily (Italy) were studied by means of neutron tomography. This was done with the aim to visualize and to measure the inner structures of the objects. In this way information about the manufacturing processes in the 16th century and the conservation status from the inside of the bronze sculptures was gained. Inscriptions found under the corrosion layer of the lead ingots gave hints about the trade routes in the past. Neutron imaging was proven perfect to transmit the relatively thick layers of Pb and Cu alloys while ceramic remains, soldering connections and corrosion effects become visible.

Electronic supplementary material The online version of this chapter (doi:[10.1007/978-3-319-33163-8_2](https://doi.org/10.1007/978-3-319-33163-8_2)) contains supplementary material, which is available to authorized users.

E.H. Lehmann · M. Estermann · S. Hartmann
Paul Scherrer Institut (PSI), 5232 Villigen, Switzerland

R. van Lang
Rijksmuseum, Amsterdam, The Netherlands

F. LoCelso
DiFC, University of Palermo, 90128 Palermo, Italy

N. Kardjilov (✉)
Helmholtz-Zentrum-Berlin, Hahn-Meitner-Platz 1, 14109 Berlin, Germany
e-mail: kardjilov@helmholtz-berlin.de

P. Tisseyre · S. Tusa
Soprintendenza del Mare della Regione Siciliana, Sicily, Italy

2.1 Introduction

The non-destructive investigation of metal objects in their full length of several centimeters is quite difficult task. The metals are strong absorbers of all kinds of ionizing radiations like X-rays, electrons and protons therefore the investigation methods using these rays are limited to surface applications. High-energy gamma rays can penetrate thick layers of metal but they are insensitive to organic inclusions and thin corrosion films. In opposite the low-energetic thermal neutrons penetrate easily centimeters of metal and are sensitive to hydrogenous substances. The non-destructive investigation of metallic cultural heritage objects like bronze or lead sculptures by neutron based methods provides very impressive results. Here we are presenting two imaging studies of metallic cultural heritage objects.

2.2 Used Experimental Methods

2.2.1 Neutron Tomography (NT)

The aim of the studies is the non-invasive analysis of the whole sample volume with the inherent spatial resolution of the tomography setup (Fig. 2.1). The contrast of the objects is given by the interaction probabilities of thermal neutrons for the material composition and the thickness of the material layer in beam direction. The cross-sections of the attenuation process are well known and tabulated (e.g. (Neutron attenuation)) and can be used for the quantitative data analysis.

The NT process is based on angular equidistant projections of the object when it is rotated around its vertical axis over the range of at least 180° (Banhart 2008; Schillinger et al. 2000). Since the neutron beam is not perfectly parallel but slightly conical it is preferred to sample over the full 360° . The number of projection defines the data quality (signal to noise) and the spatial resolution in the 3rd dimension.

After the data normalization (including open beam correction) and cleaning of “white spots” (caused by gamma events hitting the camera sensor) the projection data are ready for the reconstruction step. We used the common “filtered back-projection algorithm” which is based on the Fourier slice theorem, implemented in commercial software tools like “Octopus” (Octopus). In this manner, a stack of horizontal slices with the same pixel size of the projection data is produced which represents the whole voxel volume as the values of attenuation coefficients.

The reason why the X-ray tomography fails for bulky metallic samples is explained by the attenuation of the constituents of the objects. In Fig. 2.2 we compare the cross-section data, based on relevant libraries (Neutron attenuation, X-ray attenuation). The 100 keV X-rays compares to the spectral average of a medical X-ray tube with 180 keV high voltage. Although higher X-ray energies enable slightly higher transmission, beam hardening and scattering artifact are increased and disturb the image data quality. Therefore, it is justified to perform this kind of studies preferentially by means of NT, see Banhart et al (2010).

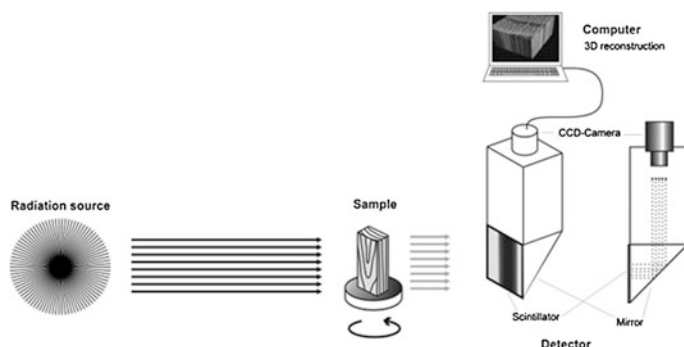


Fig. 2.1 Principle setup of the NT experiments, simplified with respect to dimensions and components, see more details in Kardjilov et al. (2011a) (courtesy D. Mannes, PSI)

More information related to the neutron radiography and tomography techniques can be found in Chap. 16 and in the following references Lehmann et al. (2005), Kardjilov et al. (2006), Lehmann et al. (2007), Kardjilov et al. (2008), Strobl et al. (2009), Lehmann et al. (2010), Kardjilov et al. (2011c).

2.3 Examples of Studies of Metal Objects by Neutrons

2.3.1 *Renaissance Bronze Objects from Rijksmuseum Amsterdam*¹

2.3.1.1 Description of the Investigated Artifacts

The artifacts which were investigated by neutron tomography are listed in Table 2.1 providing some basic information about the sculptures.

The composition of the bronze is not in all cases precisely known. The main constituents are Cu, Sn, Zn with traces of Pb.

2.3.1.2 Scientific Questions

During the long shutdown and restauration period of the Rijksmuseum Amsterdam (2003–2013) where no access by the public to the collections was possible the idea came up to perform dedicated studies of relevant bronze objects from the renaissance period in order to get information about inner compositions, manufacturing and restauration principles and about the casting processes in the 16th century.

¹Section written by E.H. Lehmann, R. van Lang, M. Estermann, S. Hartmann.

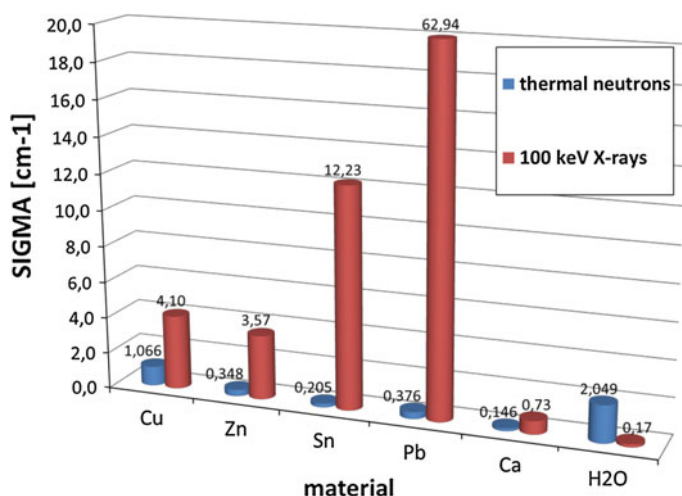


Fig. 2.2 Comparison of attenuation coefficients for the different compounds of bronze (water for comparison, symbolizing corrosion or wax, lacquer)

The two initiators of this campaign from that museum (R. van Lang, F. Scholten) were interested in non-destructive or even non-invasive investigations, partly driven by the idea of a concluding PhD thesis on that study by van Lang (2012). Their background is the restauration science and technology where the casting procedures and the finishing procedures in that time play an important role.

First radiography tests of objects by means of high-energy X-rays resulted in the conviction that the thick layers of alloys from copper, zinc, tin or even lead are hard to transmit due to the high attenuation of these materials. Therefore, it was considered better to use neutrons, in particular thermal neutrons for the transmission investigations. Since no neutron imaging facility is available and operational in the Netherlands, Belgium or Northern Germany the request for investigations was sent to PSI, where the techniques of neutron imaging are well established on an advanced level.

Thermal neutrons have the advantage of higher transmission through heavy metals than X-rays and enable even tomography studies for whole objects since the beam diameter is more than 30 cm. In NT, the three-dimensional material distribution is obtained where the dimensions, the composition, the structure, inner and outer surfaces and material failures can be extracted and analyzed. For this purpose, the object has to be rotated around its vertical axis while projects are taken from different viewing angles.

Here, we report about 14 successful investigations of objects from the Rijksmuseum's collection. About 500 years after their manufacturing it is now possible to get a virtual data volume of the samples which can be manipulated and analyzed with suitable software tools. Next to dedicated slices through the samples, extraction of different metal and ceramics structures, a full animated fly around and

Table 2.1 Information about the observed objects as far as they are available

Object	Artist	Life date	Production date	Place	Height (cm)	Inv. Nr.
Bust of a man	Severo Calzetta da Ravenna	1465/1475–1538	1458–1516	Padua or Ravenna	15.5	BK-NM-12080
Grotesque Animal	Arent van Bolten?	c. 1600			8.5	BK-1969-4
Grotesque Animal	Arent van Bolten	1573–1633	1620	Amsterdam or Zwolle	17	BK-16127
Hercules and Antaeus		1500		Padua	22.4	BK-1959-5
Mercury	Hendrick de Keyser	1565–1621	1611	Amsterdam	32.3	BK-1959-61
Nessus and Deianeira	Caspar Gras	1585–1674	1640–1650	Insbruck	33	BK-16508
Paris	Workshop Severo da Ravenna		1525	Ravenna or Pedua	26.5	BK-1959-4
Perfume burner	Desiderio da Firenze	1532–1545	1540	Veneto	40.5	BK-1957-3
She-Wolf with Romulus and Remus				Rome or Florence	11.5	BK-1958-39
Sol (The Sun)	Johan Gregor van der Schardt	1530–1581	1570–1581	Nuremberg	45.7	BK-1977-24
Striding Nobleman		1580–1600			35	BK-16083
Tiber	Tiziano Aspetti, called Mimio	1511/12–1552		Pesaro or Urbino	20 * 24 * 14	BK-1954-44
Venus holding an apple	Niccolo Roccatagliata	1560–1636	1600	Venice	14	BK-16942
Hercules Pomarius	Wilhelm van Tetrode	1525–1580	1562–1567		39.3	BK-1954-43

through the object can be delivered. Some animations are available in the e-book version of the volume as well as online through the links given to each figure.

2.3.1.3 Experimental Setup

For the investigation of the bronze sculptures the end position of the thermal neutron imaging station NEUTRA² at the Paul-Scherrer-Institute, Switzerland, was used, where a beam diameter of 35 cm circular and homogeneously illuminated was applied. The neutron spectrum can be approximated by a Maxwellian with a mean energy of 25 meV, corresponding to 1.8 Å. The collimation of the beam is characterized by an L/D-ratio of 550, corresponding to a divergence angle of 0.01°. The gamma content of the tangential beam is low and can be ignored since the detector is not much sensitive for this kind of radiation.

The detector is based on a CCD camera (ANDOR Icon-M, cooled to −50 °C for background and dark-current reduction. It observes the emitted light from a neutron sensitive scintillator screen (⁶LiF + ZnS, 0.2 mm thick) which is arranged perpendicular to the beam within a light-tight box. With the neutron intensity at the sample position of $5 \times 10^6 \text{ cm}^{-2} \text{ s}^{-1}$ the exposure time was on the order of 20 s per individual projection image.

At the time of the study, the pixel number of the CCD chip was 512 only, the resulting file was 2 Mbytes and the corresponding volume data set about 1 GByte. With the full field-of-view of 35 cm the pixel size was on the order of 0.35 mm. This relatively coarse scanning mode limits the spatial resolution (now 2048 pixels = 4 times higher resolution are common), but the major features of the objects can seriously be derived.

For the volume reconstruction step, next to the 365 projections, we took “open beam” and “dark field” images. The “open beams” were important to correct for the non-uniformity of the neutron beam, of the scintillator screen and of the CCD sensor. The “dark current” was taken to correct for the CCD off-set and other background features. In advance to the real volume reconstruction all obtained images have to be cleaned against “white spot” features, which occur if secondary radiation (mainly gammas) hit the CCD sensor. They cannot be avoided completely in neutron imaging experiments, but only reduced by some shielding and a clever arrangement of the detector with respect to the beam and the object. A perpendicular detector setup (Fig. 2.1) with a mirror between scintillator and camera has been proven to be the best solution.

²Neutron instruments are presented and described in Part II “Experimental methods”.

2.3.1.4 Results and Interpretation

Although the whole volumes of voxels are available for each object, the following data treatments were done to derive important information: outer views for comparison to photos, views of inner structures, including empty spaces, search for additional material regions next to the bulk structure, views into the often sealed inner volumes. Not in all cases important findings can be reported. However, the data material is also accessible for future more detailed studies, handed over to the museums experts. In this paper, we can show only a few images per object for the documentation of the work done.

General Observation Strategy

The three-dimensional data sets of the objects consist of values of the attenuation coefficients which are obtained by the inverse of the Beer-Lambert's law:


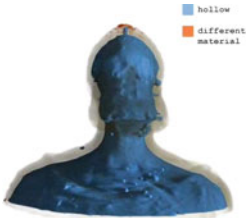

$$\Sigma = \ln\left(\frac{I_0}{I}\right)/d \quad (2.1)$$

Here, the intensities of the neutron beam in advance I_0 and behind the object I , with the sample thickness d are compared. Indeed the data set of the object is connected with the attenuation coefficient $\Sigma(x, y, z)$ or with the voxel index Σ_{ijk} , while the index numbers are given by the detector properties, e.g. the number of pixels of the sensor: between 512 and 2048.

Outside the object the attenuation values should be 0 (by definition). Inside the objects, different materials can be distinguished and separated if the differences in the attenuation coefficients are above the noise level. In the typical histogram of the Σ values we can see individual peaks which correspond to the different involved materials which can be separated by software means.

During our studies, we were able to separate and to visualize the following features: bulk metals, soldering and welding joins, repair work with other materials, resin or lacquer, ceramic remains from the casting process, inner structures for the stabilization during and after the casting process. These features will be discussed below individually for the different objects in detail.

Results from the tomography investigations of the objects listed in Table 2.1

Photo or preview	Homogeneity	Cross sections
<i>Men's head</i> 		


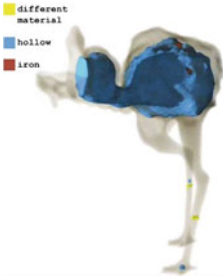
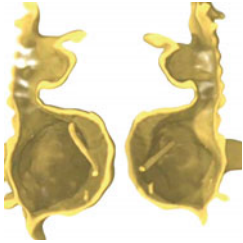
The inner volume of the object seen on the right photo is highlighted in the middle image (**in blue**), indicating the regions of the inner surface and some empty pores in the bulk. This is compared to the virtually sliced object on the right side. Obviously, on the heads peak some other (sealing?) material (**in red**) can be found closely connected with the filling channel remained in that region

Video: https://youtu.be/_mMSrHXzPb8

<i>Grotesque 1</i> 		
--	--	---

The transparent view (middle) and the virtual cut (right) verify casting mistakes/porosity (**in blue**) in the bulk of the sample and traces of wax/lacquer (**in red**) on the surface. No casting core is visible

Video: https://youtu.be/P7ejI_BT2Tw




<i>Grotesque 2</i> 		
---	---	---

The empty space of this hollow casted sample is shown in the middle image (**in blue**), the inner surface and some stabilizing wires can be seen in the slices in the right figure. Some iron traces (**in red**) and different materials (**in yellow**) can be seen in the transparent structure in the middle image


Video: <https://youtu.be/F5gud6Mql7U>

(continued)

(continued)

Photo or preview	Homogeneity	Cross sections
<i>Hercules and Anteaus</i> 		




Whereas the lower figure is cast hollow (**in blue**), the “upper” body is filled with another material (**in red**), probably ceramics from the casting process; the tomography data show some outer damages of the lower figure, e.g. at the knee (middle image). The slices through the bodies (right image) show in detail the hollow areas, the remaining casting residuals and the non-homogeneities in the metal structure
Video: <https://youtu.be/WRPBFJnb5y8>

<i>Mercury</i> 		
--	--	---

These perspectives document well the empty areas (**in blue**) in the sculpture where the ceramic core was (partly) removed (middle image). In the bust region another material can be seen (**in yellow**) indicating some repair work or the filling point during casting, closed later. These cuts in the right image show the bronze material distribution inside the object. There is a clear separation line on half height of the body and numerous larger pores in the bulk. Some remaining core material is also visible
Video: <https://youtu.be/E9dEFWYcy98>

(continued)

(continued)

Photo or preview	Homogeneity	Cross sections
<i>Nessus and Deianeira</i> 		

The sculpture has large areas of emptiness (**in blue**), in particular within the riding person and the horse body. The cut demonstrates that the empty regions are stabilized by sticks and wires also made of metallic structures

Video: <https://youtu.be/xY4Z36QblUA>




<i>Paris</i> 		
--	--	--

Nearly the whole upper body is empty (**in blue**) whereas some different material (**in red**) can be found at the lower right leg. The hollow structure of the object is verified, the casted layer is solid and without voids or pores, some stabilizing cables can be seen near the shoulder. The legs are fully cast in metal, casting remains are mostly removed

Video: <https://youtu.be/YRdKmlOBEN8>

(continued)

(continued)

Photo or preview	Homogeneity	Cross sections
<i>Sol</i> 		

Half of the human body and that of the lion is emptied (**in blue**). In both parts of the sculpture the remaining casting core can be found with a different contrast compared to the metallic shape
Video: <https://youtu.be/EwCXQ0ZLNVY>





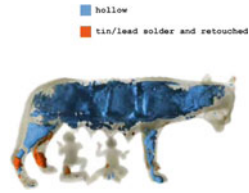

<i>Striding Nobleman</i> 		
--	--	--

The object is mainly hollow (**in blue**), but the legs are separately added in a soldering process, the fixing point at the ground plate are made from a different material. These views demonstrate the components inserted to stabilize the structure of the object while the variable wall thickness can also be seen

Video: https://youtu.be/rPM_kS8Zodg


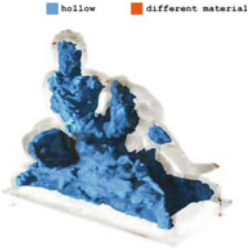

(continued)

(continued)

Photo or preview	Homogeneity	Cross sections
<p><i>Perfume</i></p> 		
<p>While the man on top of the object is cast solid, the figures on the lower level are all empty (in blue). The structure through the metallic layers and all material distribution in the object can be derived from these slices Video: https://youtu.be/IPfSNfJd1fU</p>		
<p><i>She-wolf with Romulus and Remus</i></p> 		
<p>The wolfs body is mainly hollow (in blue), some additional material can be seen in the legs (ceramic remains in red); the two kids are casted solid Video: https://youtu.be/45LKr_E29BM</p>		

(continued)




(continued)

Photo or preview	Homogeneity	Cross sections
<p><i>Tiber</i></p> 		

The sculpture has a big hollow volume marked **in blue**

Video: <https://youtu.be/mTc8XuHIBSY>

Venus holding an apple




		
--	--	--

This sculpture is more or less solid with only a few empty areas (**in blue**). Around the head and the arm some additional material (**in red**) can be found, probably from repair work. The regions with higher material porosity can be seen in these virtual slices in detail

Video: <https://youtu.be/LfwtwC044iU>

(continued)

(continued)

Photo or preview	Homogeneity	Cross sections
<i>Hercules Pomarius</i> 		

Nearly the whole body is empty (**in blue**), only in the legs and arms some remaining material (**light gray**) from casting can be found. The semitransparent view indicates the material distribution

2.3.1.5 Concluding Remarks Related to the Investigation of Bronze Objects

The presented data of the 14 objects from the collection of Rijksmuseum Amsterdam verified that a non-invasive investigation of even bulky bronze objects is possible by NT methods. In particular, thermal neutrons have much higher penetration ability than X-rays. For the current set of samples we did not register strong artifacts by the sample scattering like beam hardening in the X-ray case.

It was possible to distinguish between inner cavities, ceramic casting remains and the pores distribution in the bulk. In addition, some stabilization reinforcement parts inside the objects were identified. Measures of restauration become visible as areas with a different neutron contrast.

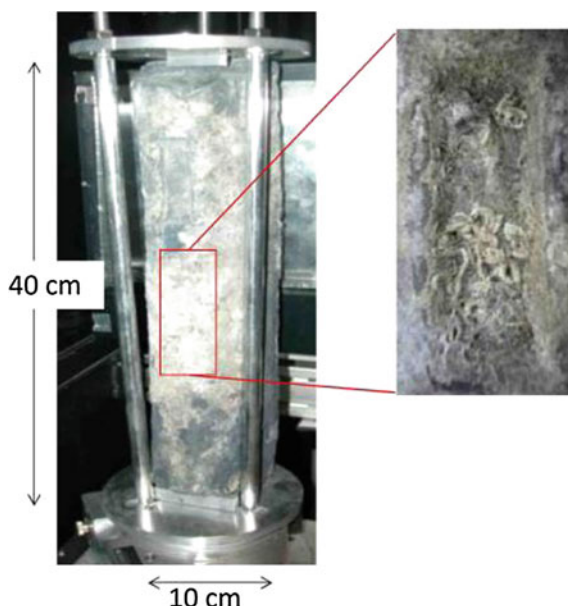


Fig. 2.3 Lead ingot from Siracusa in the experimental sample holder. The *zoomed region* refers to the *middle* cartouche (Triolo et al. 2014—Reproduced by permission of The Royal Society of Chemistry)

2.3.2 Shipwrecks Keep Invaluable Treasures³

2.3.2.1 Description of the Investigated Artifacts

Ancient roman lead ingots (3rd–1st century BC) were investigated by NT. The ingots are belonging to sunken roman ships in two different locations near Sicily's coast.

In the first location (Siracusa, Italy ca. I BC) 4 similar lead ingots were found under water. They have the same troncopyramidal shape, length of about 40 cm and same weight of ca. 33 kg (the maximum weight a slave could carry by the Roman law) as well as a rectangular mold mark on the top side. In Fig. 2.3 one of these ingots is shown in the specially developed holder which allows for rotation of the sample around its vertical axis.

The photography of the ingot in Fig. 2.3 shows that its surface is heavy damaged due to deposits of salts, algae and probably carbonaceous material, very likely coming from a fire occurred on the ship. The ingots are usually characterized by mold marks located in three regular indented rectangular areas (cartouches) where both characters and images are found. In this sample these areas of interest are

³Section written by F. LoCelso, N. Kardjilov, P. Tisseyre, S. Tusa.



Fig. 2.4 Picture of the whole lead ingot depicting its highly damaged state, concretions are clearly observable. It is also marked (*red square*) the area in one of the slanted sides where signs were found after the digital reconstruction (Triolo et al. 2014—Reproduced by permission of The Royal Society of Chemistry)

covered by deposit and in the middle section, one could see a hint of an image (zoomed region in Fig. 2.3).

Another kind of lead ingot was found in a second location in Capo Rasocolmo Messina (Italy) that could be probably date back to the 3rd century BC, as shown in Fig. 2.4. It has different shape in the cross section, different length and weight (length of 35 cm and weight of ~ 30 kg) compared to the one described in Fig. 2.3.

2.3.2.2 Scientific Questions

Lead was a basic material in the Roman age between 2nd century BC and the 1st century AC which was used in ship construction, both military and commercial, as well as in pipe systems for water and wastewater management. The Mediterranean Sea played an important role in the lead trading where the raw material was transported in form of ingots by commercial ships. Therefore the study of the ship wrecks on the sea ground and the characterization of rescued lead ingots are very important in showing us the net of ancient commercial trade routes.

The NT imaging technique is very suitable for the non-destructive investigation of corroded lead objects due to the high penetration power of the neutron radiation (lead is notoriously opaque to X-rays). The obtained digitalized volume can be processed by 3D volume rendering software which helps, for example, to remove digitally the corrosion layer and in this way to visualize the original surface of the sample. The final results of the epigraphic analysis will provide useful insights about the producer, the origin and the age of the finding.

2.3.2.3 Experimental Setup

The experiments were performed at the neutron imaging facility CONRAD⁴ at Helmholtz-Zentrum Berlin, Germany. The facility is situated at the end of a curved

⁴Neutron instruments are presented and described in Part II “Experimental methods”.

neutron guide facing the cold source of the BER-II research reactor (Kardjilov et al. 2011b). The neutron guide provides a cold neutron flux in the order of app. 2×10^8 n/cm² s directly at the end of the guide with a negligible background of γ -radiation and fast neutrons. A pinhole geometry with L/D of 170 (L = 500 cm, D = 3 cm) was used for achieving of better spatial resolution within a beam field of 10 cm \times 10 cm with a neutron flux of $\sim 10^7$ n/cm² s. The used detector system was based on a 16-bit CCD camera (Andor) with 2048 \times 2048 pixels. The images obtained from the LiZnS scintillator are projected via a mirror and a lens system onto the CCD chip (Kardjilov et al. 2011a).

For the tomographic measurements 300 radiographic projections at continuing rotation angles were taken over 360°. The exposure time per projection image was 10 s and the overall time for the tomographic measurement was about 1.5 h. Due to the limited field of view of 10 cm \times 10 cm the sample was measured only at 3 heights where the stamps were located. For samples without visible signs on the surface the whole sample length was scanned with vertical steps of 10 cm (4 tomographies in total). The data were reconstructed with a backprojection algorithm implemented in the software Octopus (Octopus). For visualization and 3D rendering the software VGStudioMax was used (Volume Graphics). After the illumination of the samples by the neutron beam the irradiated parts become radioactive. However after some decay time the samples were approved to be non-radioactive again. In our case the necessary decay time was about 3 days.

2.3.2.4 Results and Discussion

The NT reconstruction of the three cartouches of the lead ingot of Fig. 2.3 (see Fig. 2.5) shows, in the middle section, that the image found represents a dolphin. This fact is indeed consistent with the finding, in the two cartouches adjacent to the dolphin figure, of two different inscriptions in relief, as shown in Fig. 2.5 (top and bottom part). They read as MPLANILF, i.e. M(arcii) PLANI(i) L(ucii) F(ilii), and RVSSINI (Russini) respectively, accordingly to the tria nomina standard used mainly by Roman citizen (Domergue 1987). Indeed they were identified by a personal name, i.e. the praenomen (Marcius in its genitive form), followed by the family name, i.e. nomen (Planus in its genitive form) and then a third name, i.e. cognomen (Russini), which basically indicates a specific branch of the family. This epigraphic analysis refers therefore to the producer of the lead ingots and possibly also the mine owner in Carthago Nova in Spain (Trincherini et al. 2010; Tisseyre et al. 2008) which dates back to 1st century BC, when in fact the Planius family (either Marcius or Lucius, probably brothers and sons of Lucius, as the L(ucii) F(ilii) inscription suggests) was active in lead ingots trading. In fact the latter were found in ship wrecks in many locations along the coast of Italy and France.

Similar characteristics were found in the other three ingots which at naked eye also appear to have partially erased mold marks. The second lead ingot, as shown in Fig. 2.4 has not only different shape in the cross section compared to the one described in Fig. 2.3, but also different length and weight (length of 35 cm and

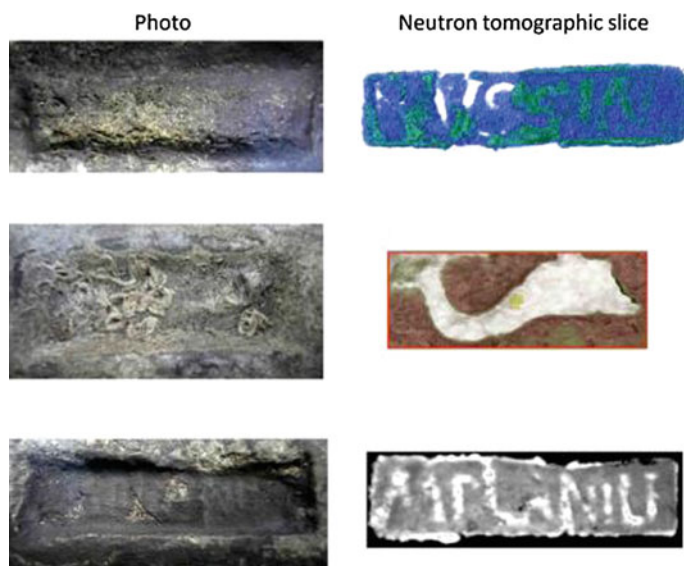


Fig. 2.5 Comparison between the three cartouches of lead ingot of Fig. 2.3; *on the left* the naked eye view, *on the right* the corresponding digitally reconstructed images (Triolo et al. 2014—Reproduced by permission of The Royal Society of Chemistry)

weight of ~ 30 kg). This ingot was a part of a load rescued in Capo Rasocolmo Messina (Italy) that could be probably date back to the 3rd century BC. It is possible to see that it has slanted sides and a rounded top while the base is still rectangular. The sample is heavily covered by calcareous concretions which in some parts include small spherical shaped stones (see the protrusion in the lower right part of Fig. 2.6b). There are two regions of interest, beneath the calcareous concretion in one of the slanted sides. It is possible to see, in the right part of Fig. 2.6a, a big X shaped sign running across the whole width of the ingot, while about 10 cm away, in the left part of the digital reconstruction, there is a group of characters which could lead to a possible identification of the maker.

The group of characters can be read as CP which can be probably traced back to one of the Cartagena's producers C(aius) P(ontileieni) which is contemporary to the Planius family. Indeed it has been found around 3rd century BC (Laubenheimer-Leenhardt 1973) that some of the Ingots produced by the Planius family have been stamped as well with Marcus Caius Pontilieni inscription. The big X shaped sign is probably a mark for the production or trade control. In Fig. 2.6b it is also shown in the vertical projection that the letters have been stamped; the depth of the stamp is 4.7 mm and it is triangularly shaped.

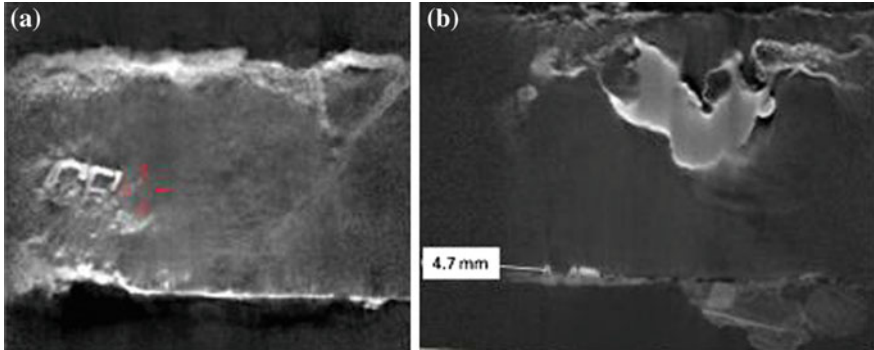


Fig. 2.6 **a** From the digital reconstruction a group of two letters as well as a big cross sign (not visible at naked eye) were found. The *red mark* on the image is showing the position of the cutting plane for the cross section shown in subsection **b**; **b** top view of the slanted side where the letters were found showing the shape and the depth of stamping marks (Triolo et al. 2014—Reproduced by permission of The Royal Society of Chemistry)

2.3.2.5 Concluding Remarks Related to the Study of Lead Objects

The results presented here give an insightful perspective on the possibilities offered by NT in the field of archeological investigations. The technique has been applied on severely damaged lead ingots rescued from underwater shipwrecks, and it has given final answers both on the provenance and the historical frame time in which the ingots were traded. It is very important to underline that this experimental technique allowed not only to examine rather bulky samples, but thanks to its selectivity to different elements it also made possible to digitally retrieve precious information in a non-destructive way.

Table 2.2 Conditions for activation of bronze compounds by bombardment with thermal neutrons

Material	Isotope	Content (%)	Capture CS [barn]	Resulting nuclide	Half life
Cu	Cu-63	69.17	4.506	Cu-64	12.7 h
	Cu-65	30.83	2.168	Cu-66	5.12 min
Zn	Zn-64	48.60	0.76	Zn-65	224.3 days
	Zn-68	18.80	1.073	Zn-69	13.76 h
	Zn-70	0.60	0.091	Zn-71	2.45 min
Sn	Sn-120	32.59	0.14	Sn-121	27.06 h
	Sn-122	4.63	0.18	Sn-123	129.3 days
	Sn-124	5.79	0.13	Sn-125	9.64 days
Pb	Pb-204	1.40	0.66	Pb-205	5.54 ms
	Pb-208	52.40	0.0005	Pb-209	3.25 h

2.4 Final Thoughts

There were some doubts about the activation of the bronze and lead samples during the neutron exposure. In Table 2.2 the capture cross-sections of the relevant isotopes in the observed materials and the half-lives of the exited nuclei can be found. The only relevant isotope is Cu-63 due to the relatively long half-live and a unneglectable capture cross-section.

Indeed, just after exposure there is some emission of secondary radiation due to the decay of activated nuclides. However, the involved material activity is short-living and the background level is reached after about 3 days at most. This is confirmed by the practical radiation measurements at real samples by experts. Materials like Co or Ag should be avoided to be studied since their half-lives are too long and the activation rate high. In the current study, there is no such material involved.

References

- Banhart J (ed) (2008) Advanced tomographic methods in materials research and engineering. Oxford University Press, Oxford, UK
- Banhart J, Borbely A, Dzieciol K, Garcia-Moreno F, Manke I, Kardjilov N, Kaysser-Pyzalla AR, Strobl M, Treimer W (2010) X-ray and neutron imaging—Complementary techniques for materials science and engineering. *Int J Mater Res* 101:1069–1079
- Domergue C (1987) Les lingots de plomb de l' épave romaine de Valle Ponti (Comacchio). *Epigraphica* 49:109–175
- Kardjilov N, Fiori F, Giunta G, Hilger A, Rustichelli F, Strobl M, Banhart J, Triolo R (2006) Neutron tomography for archaeological investigations. *J Neutron Res* 14:29–36
- Kardjilov N, Hilger A, Manke I, Benfante V, Lo Celso F, Triolo R, Ruffo I, Tusa S (2008) Neutron tomography in modern archaeology. *Notiziario Neutroni e Luce di Sincrotrone* 13:6–9
- Kardjilov N, Dawson M, Hilger A, Manke I, Strobl M, Penumadu D, Kim F, Garcia-Moreno F, Banhart J (2011a) A highly adaptive detector system for high-resolution neutron imaging. *Nucl Instrum Methods Phys Res, Sect A* 651:95–99
- Kardjilov N, Hilger A, Manke I, Strobl M, Dawson M, Williams S, Banhart J (2011b) Neutron tomography instrument CONRAD at HZB. *Nucl Instrum Methods Phys Res, Sect A* 651:47–52
- Kardjilov N, Manke I, Hilger A, Strobl M, Banhart J (2011c) Neutron imaging in materials science. *Mater Today* 14:248–256
- Laubenheimer-Leenhardt F (1973) Recherches sur les lingots de cuivre et de plomb d'époque romaine dans les régions de Languedoc-Roussillon et de Provence-Corse, Paris ed. de Boccard 1973
- Lehmann E, Hartmann S, Wyer P (2005) Neutron radiography as visualization and quantification method for conservation measures of wood firmness enhancement. *Nucl Instrum Methods Phys Res, Sect A* 542:87–94
- Lehmann E, Vontobel P, Frei G (2007) The non-destructive study of museums objects by means of neutrons imaging methods and results of investigations. *Nuovo Cimento Della Societa Italiana Di Fisica C (Geophys Space Phys)* 30:93–104
- Lehmann E, Hartmann S, Speidel MO (2010) Investigation of the content of ancient Tibetan metallic Buddha statues by means of neutron imaging methods. *Archaeometry* 52:416–428

- Mouchot D (1970) Pièces d'ancres, organeaux et ornements de plomb antiques découverts entre Antibes et Monaco. *Rivista di studi liguri* 36:307–318
- Neutron Attenuation. Available: <https://www.ncnr.nist.gov/instruments/bt1/neutron.html>
- Octopus. Available: <http://www.inct.be/en/software/octopus>. Accessed 12 Oct 2015
- Schillinger B, Lehmann E, Vontobel P (2000) 3D neutron computed tomography: requirements and applications. *Phys B* 276–278:59–62
- Strobl M, Mankie I, Kardjilov N, Hilger A, Dawson M, Banhart J (2009) Advances in neutron radiography and tomography. *J Phys D-Appl Phys* 42:243001
- Tisseyre P, Tusa S, Cairns WRL, Selvaggio Bottacin F, Barbante C, Ciriminna R, Pagliaro M (2008) *Oxford J Archaeol* 27:315–323
- Trincherini PR, Domergue C, Manteca I, Nesta A, Quarati P (2010). [arXiv:1002.3557](https://arxiv.org/abs/1002.3557)
- Triolo R, Lo Celso F, Tisseyre P, Kardjilov N, Wieder F, Hilger A, Mankie I (2014) Neutron tomography of ancient lead artefacts. *Anal Methods* 6:2390–2394
- Van Lang R (2012) Technical studies of Renaissance bronzes. Dissertation TU Delft. ISBN 978-90-71450-49-5
- Volume Graphics. Available: <http://www.volumegraphics.com/> (accessed)
- X-ray Attenuation. Available: <http://www.nist.gov/pml/data/xraycoef/>

Neutron Methods for Archaeology and Cultural Heritage

Kardjilov, N.; Festa, G. (Eds.)

2017, X, 349 p. 181 illus., 127 illus. in color., Hardcover

ISBN: 978-3-319-33161-4